

Predictability of stationary and non-stationary internal tides in the US Navy global hydrodynamical model

Brian K. Arbic¹, Maarten C. Buijsman² Eric P. Chassignet³ Thomas W.N. Haine⁴ Hans E. Ngodock⁵ James G. Richman³ Jay F. Shriver⁵ Innocent Souopgui⁶ Xiaobiao Xu³

6/4/2020-5/31/2024

¹University of Michigan ²University of Southern Mississippi ³Florida State University

⁴Johns Hopkins University ⁵Naval Research Laboratory ⁶University of New Orleans

NASA award number 80NSSC20K1135

Overview and objectives

In this project we will examine the predictability of stationary and non-stationary internal tides in the US Navy global hydrodynamical system, which is built upon 1/12.5 and 1/25 degree global simulations of the HYbrid Coordinate Ocean Model (HYCOM; e.g. Chassignet et al. 2009), and which include simultaneous atmospheric and tidal forcing (e.g., Arbic et al. 2010). By “stationary” internal tides, we mean tides that can be written in terms of a sine wave, with an amplitude and a phase; hence, perfectly predictable. By “non-stationary” internal tides, we mean internal waves in the tidal band that cannot be written in terms of an amplitude and a phase; in other words, the non-stationary internal tides represent what is left over in the tidal band after the stationary internal tides have been removed. The HYCOM tidal simulations contain the oceanic general circulation, mesoscale eddies, barotropic tides, internal tides and a partially resolved internal gravity wave (IGW) continuum (e.g., Arbic et al. 2018). Interactions with eddies, and a stratification that varies in time, render a substantial fraction of the internal tide variance to be non-stationary (incoherent; e.g. Buijsman et al. 2017, Nelson et al. 2019). The HYCOM prediction system uses the Navy Coupled Ocean Data Assimilation (NCODA) scheme (Cummings 2005), which assimilates the locations and amplitudes of eddies in satellite altimeter data. An Augmented State Ensemble Kalman Filter (ASEnKF), that uses perturbations having length scales typical of those in open-ocean barotropic tides, is used to improve the accuracy of those tides (Ngodock et al. 2016).

We will test the degree to which the assimilative model can predict the stationary internal tide sea surface height (SSH) variance in some internal tide hotspot regions, such as Hawai’i, the French Polynesian Islands, and others. We will strive to improve the accuracy of the modeled barotropic tides with an ASEnKF that includes additional perturbations focused on regions of large resonant coastal tides, with smaller horizontal scales resembling those of the coastal tides. We will also test improvements to the modeled barotropic tides resulting from the addition of newer bathymetric datasets. Finally, improvement of the HYCOM system is likely to come from assimilation of SWOT data itself, which will two-dimensional, high-resolution observations of SSH.

In addition to our tests of stationary internal tides in the model, we will also determine whether nadir and SWOT SSH variance in the semidiurnal band is reduced when corrected by the HYCOM semidiurnal band-passed SSH, which includes non-stationary as well as stationary internal tides. In other words, we will test whether HYCOM has skill in removing non-stationary internal tides; a test that has been put forward as a “grand challenge” for the SWOT project.

Our work is relevant for SWOT because accurate corrections for internal tides must be made in order for smaller-scale low-frequency motions such as mesoscale and submesoscale eddies to be clearly observed in SWOT observations (e.g. Richman et al. 2012, Rocha et al. 2016, Savage et al. 2017, amongst many).

We will also feed global SSH output, and three-dimensional output in the SWOT Cal/Val region, from operational HYCOM to other project members. Our HYCOM output is likely to be especially important during the Calibration/Validation (Cal/Val) phase of SWOT. We will run non-assimilative HYCOM on a non-Navy machine in order to make its three-dimensional output available to the community. Funds for this project will support co-Is to help with improvements in the ASENKF, improvements in a 1/50 degree North Atlantic HYCOM simulation (Chassignet and Xu 2017), and improvements in our understanding of what happens in our hydrostatic model in regions where strongly nonhydrostatic internal solitons develop. Lastly, we will continue to inter-compare the internal tides and IGWs in several global hydrodynamical internal wave models.

Approach and results

A map of the M_2 stationary internal tide SSH variance in recent free-running global 1/25° HYCOM simulations vs. estimates from altimeters is given in Figure 1. HYCOM simulates the regions of high stationary internal tide activity reasonably well; the geographical variations seen in internal tide generation “hotspots” vs. relatively quiet regions are clearly correlated between the two panels in the figure.

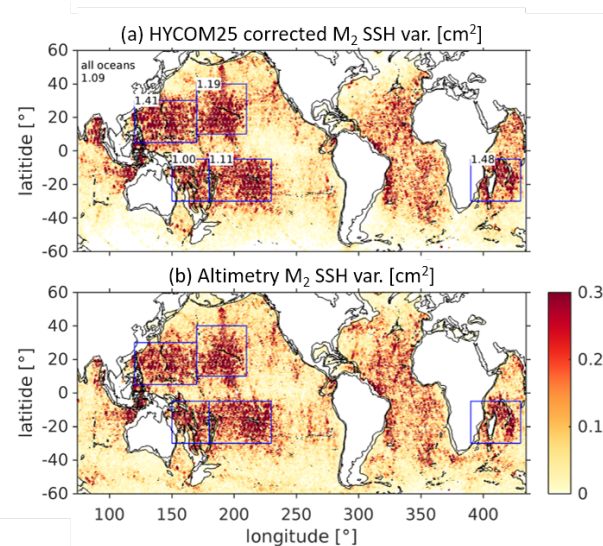


Figure 1. M_2 internal tide SSH variance in (a) simulated and corrected 1/25° HYCOM (b) altimetry (Ray and Byrne 2010). The HYCOM time series are corrected with a spatially varying correction factor (Ansong et al. 2015, Buijsman et al. 2020), which accounts for the decay of stationary variance as a function of time series duration. The numbers in (a) represent the ratio between the area-integrated HYCOM and altimetry variance for the internal-tide hotspot regions (blue boxes) and the global ocean (top left). From Buijsman et al. (2020).

We have also investigated internal tide SSH nonstationary, in HYCOM vs. satellite altimetry. Global maps in Figure 2 display the semidiurnal non-stationary variance fraction (SNVF) in a HYCOM simulation (Shriver et al. 2012) and from altimetry (Zaron 2017). The non-stationary variance is taken as the variance remaining in the spectrum after stationary internal tides have been removed. In the top plot of Figure 2, the SNVF is computed from frequency spectra of hourly HYCOM output. Because nadir altimetry data is not taken at hourly intervals, but is instead taken at intervals of about 9.9156 days, wavenumber spectra must be used to compute the SNVF from altimetry data (bottom plot, Figure 2). The model can be sampled as the real ocean is by altimeters. The second plot of Figure 2 displays the SNVF computed from wavenumber spectra applied to hourly HYCOM output. The third plot displays the SNVF computed from wavenumber spectra applied to 9.9156-day sampled HYCOM output. All four plots of Figure 2 display large non-stationarity in the eastern equatorial Pacific, consistent with the analysis of Buijsman et al. (2017). The consistency of the plots in Figure 2 gives us confidence that HYCOM tidal simulations that also include data-assimilation on eddies might be able to help remove non-stationary internal tide variance from altimeter records. We are currently testing whether HYCOM is able to remove stationary and non-stationary variance from altimeter records.

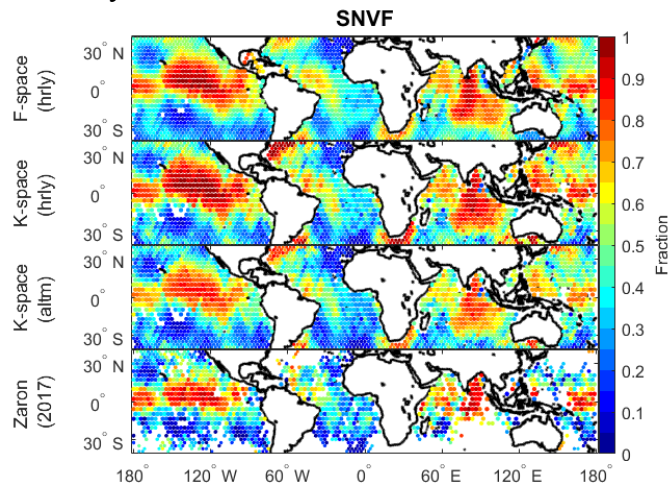
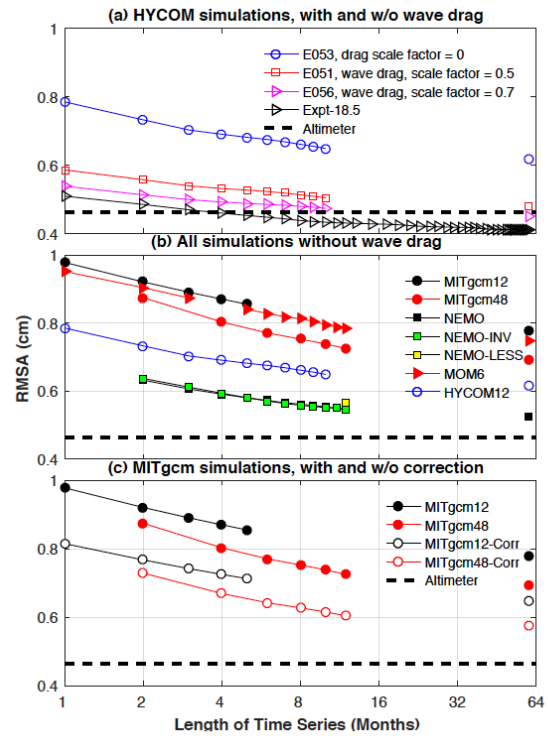


Figure 2. (left) The semidiurnal non-stationary variance fraction (SNVF) computed from (first) frequency spectra of hourly HYCOM output, (second) wavenumber spectra of hourly HYCOM output, (third) wavenumber spectra of HYCOM output sampled every 9.9156 days, (fourth) wavenumber spectra of altimeter output sampled every 9.9156 days. From Nelson et al. (2019).

Ansong et al. (2020, in preparation) is comparing the barotropic tides and internal tide SSH signatures in global simulations of $1/12.5^\circ$ HYCOM, $1/12^\circ$ and $1/48^\circ$ MITgcm, $1/12^\circ$ NEMO, and $1/12^\circ$ MOM6 with the altimeter-constrained model TPXO and along-track altimeter data, respectively. The MITgcm barotropic tides are too large, mainly because of a lack of parameterized topographic wave drag, and in part because of an inadvertently large astronomical potential in the MITgcm simulations. Comparison of the stationary internal tides in the models with altimeter observations is provided in Figure 3. As in Ansong et al. (2015) and Buijsman et al. (2020), the globally averaged stationary internal tide SSH amplitude decays as the record length expands. A long HYCOM experiment with wave drag, denoted “18.5”, is used to extrapolate the results of other simulations out to 60 months. In HYCOM simulations without wave drag (blue circles), the internal tides are too large, in comparison with observations. HYCOM results that include wave drag lie closer to observations. The internal tides in the simulations of other models, which do not include wave drag, are also too large.

Interestingly, the internal tides in MITgcm simulations run with $1/48^\circ$ horizontal grid spacing are smaller than those in $1/12^\circ$ simulations. We speculate that the smaller internal tides in the higher-resolution MITgcm simulations are due to energy loss resulting from the cascade that feeds the IGW continuum spectrum, which is more active in the higher-resolution MITgcm simulation (Rocha et al. 2016, Savage et al. 2017, Leucke et al. 2020).

Figure 3. Globally-averaged root-mean-square amplitude, RMSA, of modeled stationary M_2 internal tide elevations and along-track altimeter value versus length of time series. The x-axis is a base 2 log scale. (a) $1/12^\circ$ HYCOM results with and without wave drag (as in Ansong et al 2015). HYCOM experiment “18.5” is an older HYCOM simulation, which included wave drag and which was run out longer than the other simulations shown (5 years). (b) Results from all simulations that are without wave drag. (c) MITgcm simulations with and without a correction factor for the MITgcm simulations, which inadvertently used an overly large astronomical tidal forcing, based on work with the model of Schindelegger et al. (2018). The amplitudes shown at month 60 are rough estimates based upon changes of internal



Our NRL collaborators are preparing for the ingestion of SWOT SSH data, which is expected to greatly increase the ability of HYCOM to accurately track mesoscale eddies. The impact of additional SWOT data was investigated in twin-data assimilation experiments (Carrier et al. 2016), which showed that the SWOT observations help to constrain the model mesoscale (50–250 km) and surface velocity throughout a 96-hour forecast better than nadir altimeters alone (Figure 4).

Next, we display results (Figure 5; Nelson et al. 2020) from a regional simulation of the MITgcm, demonstrating that the IGW continuum is more fully simulated in regional models that employ boundary conditions that include low-mode internal waves radiating from far away, and model grid spacings are made finer than is possible in global models. Ultra-high-resolution regional models will be required to understand the high-resolution SSH measurements of SWOT. Nelson et al.’s results demonstrate that regional models can produce reasonably realistic IGW spectra as long as they meet the conditions described above. Nelson et al.’s results complement those of Mazloff et al. (2020), who

show that regional models that lack the internal wave boundary conditions have an insufficiently energetic IGW spectrum relative to observations.

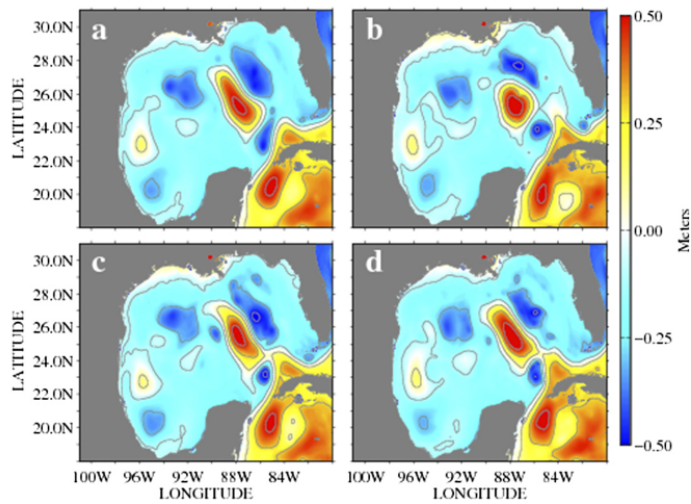


Figure 4. Model SSH (m) valid on 4 Jun 2014, for (a) the nature run, (b) ALT, (c) SWOT and (d) COM experiments. From Carrier et al. (2016).

ALT: assimilates SSH observations only from existing nadir altimeters
 SWOT: assimilates SSH observations from potential SWOT altimeter
 COM: assimilates SSH observations from both.

From Carrier et al. (2016).

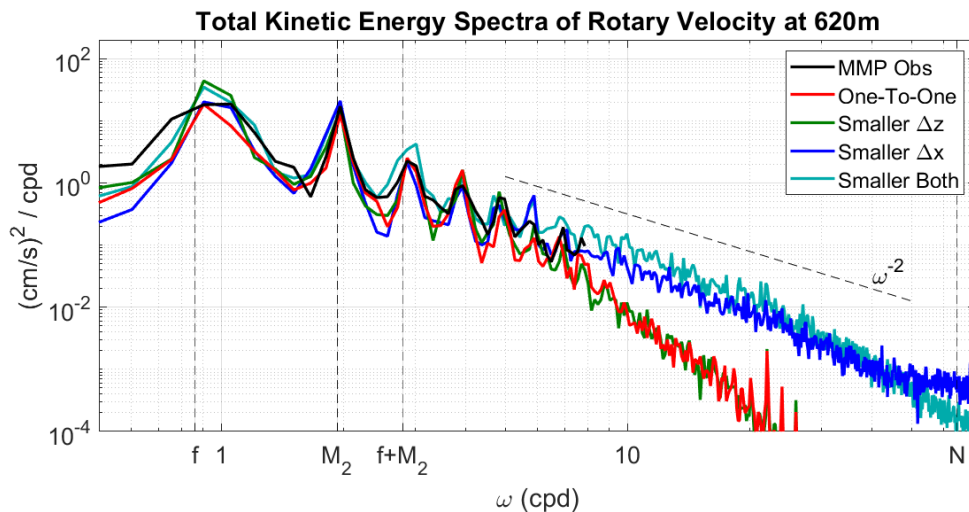


Figure 5. Frequency spectra of horizontal kinetic energy at 620 m depth, at 25°N, 195°E, in McLane Moored Profiler (MMP) observations and regional simulations of the MITgcm, run in a 6° by 8° box near Hawai’i and forced at its boundaries by the global 1/48° MITgcm. “One-to-one” indicates a simulation with the same horizontal and vertical resolutions as the parent global simulation. “Smaller delta z” indicates a simulation with a vertical grid spacing three times finer than the parent, while “Smaller delta x” has a horizontal grid spacing eight times finer, and “Smaller Both” has finer spacings in both horizontal and vertical directions. The extra dashed line denotes the expected -2 slope at high-frequencies from the Garrett and Munk (1972, 1975) model. “ f ” denotes Coriolis frequency. From Nelson et al. 2020.

We conclude by noting again that we continue to compare global internal wave models to observations as much as we possibly can. In Figure 6 we display preliminary calculations of the zonal averages of kinetic energy in the low-frequency (< 0.5 cpd), semidiurnal, diurnal, and near-inertial bands, in $1/25^\circ$ global HYCOM simulations. The figure also includes results from $1/48^\circ$ global MITgcm simulations and surface drifters, which were compared in Yu et al. (2019). The addition of HYCOM to the comparisons demonstrates that topographic wave drag can indeed bring modeled internal tides closer to observations, through parameterizing the drag and energy loss due to breaking internal waves that global models cannot resolve. The HYCOM results also demonstrate that more accurate near-inertial wave motions are obtained in models that have more frequently updated wind fields (the MITgcm simulations used 6 hourly wind fields, while HYCOM winds are updated more frequently). These types of comparisons will help to improve all the global internal wave models that will be used to interpret SWOT results.

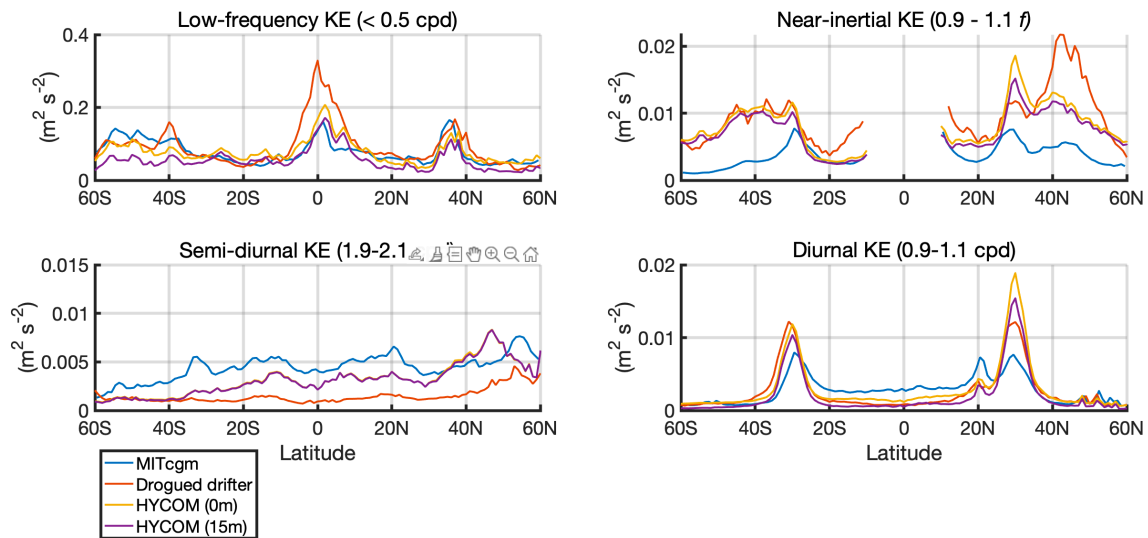


Figure 6. Zonally averaged kinetic energy from drogued drifters, the surface (0 m) of global $1/48^\circ$ MITgcm simulations, and the surface (0 m) and 15 m depth of global $1/25^\circ$ HYCOM simulations. Results are shown for low-frequency (< 0.5 cpd), semidiurnal, diurnal, and near-inertial bands. The drifter velocities represent measurements from 15 meter depth more so than the surface (Shane Elipot, personal communication, 2020); the 0 vs. 15 m HYCOM results demonstrate that the results differ slightly between these depths, though not enough to change the qualitative comparisons between the model and drifter results. Figure represents preliminary results, from a paper in preparation by Jonathan Brasch.

Expected milestones

Moving HYCOM output to the SWOT community—ongoing.

First paper on ability of HYCOM to remove stationary and non-stationary internal tide variance from nadir altimeter records—2020.

Paper on inter-comparison of several global internal tide models with altimetry—2020.

Paper on comparison of global HYCOM and MITgcm to drifter data—2020.

Participation in SWOT Cal/Val including moving HYCOM output to SWOT community—ongoing.

Ingestion of SWOT data into NRL HYCOM simulations—after SWOT launch.

Paper on comparison of HYCOM internal tides to SWOT data—after SWOT launch.

Continuing analysis of very-high-resolution regional models—ongoing.

References

Ansong, J.K., B.K. Arbic, M.C. Buijsman, J.G. Richman, J.F. Shriver, and A.J. Wallcraft, 2015. Indirect evidence for substantial damping of low-mode internal tides in the open ocean. *Journal of Geophysical Research Oceans* 120, 6057-6071, doi:10.1002/2015JC010998.

Ansong, J.K., B.K. Arbic, D. Menemenlis, A.J. Wallcraft, R. Bourdalle-Badié, J. Chanut, F. Briol, M. Schindelegger, R.D. Ray, E.P. Chassignet, A.J. Adcroft, R.W. Hallberg, L. Carrère, G. Dibarboure, N. Picot, M.C. Buijsman, J.G. Richman, J.F. Shriver, C.N. Hill, M.R. Mazloff, A.T. Nguyen, R.M. Ponte, A. Kock-Larrouy, and F. Lyard, 2020. Importance of damping in comparison of internal tides in several global hydrodynamical models with altimetry. In preparation.

Arbic, B.K., A.J. Wallcraft, and E.J. Metzger, 2010: Concurrent simulation of the eddying general circulation and tides in a global ocean model. *Ocean Modelling* 32, doi:10.1016/j.ocemod.2010.01.007, 175-187.

Arbic, B.K., M.H. Alford, J.K. Ansong, M.C. Buijsman, R.B. Ciotti, J.T. Farrar, R.W. Hallberg, C.E. Henze, C.N. Hill, C.A. Luecke, D. Menemenlis, E.J. Metzger, M. Müller, A.D. Nelson, B.C. Nelson, H.E. Ngodock, R.M. Ponte, J.G. Richman, A. C. Savage, R.B. Scott, J.F. Shriver, H.L. Simmons, I. Souopgui, P.G. Timko, A.J. Wallcraft, L. Zamudio, and Z. Zhao, 2018. A primer on global internal tide and internal gravity wave continuum modeling in HYCOM and MITgcm. In *New frontiers in operational oceanography*, E. Chassignet, A. Pascual, J. Tintore, and J. Verron, Eds., GODAE OceanView, 307-392, doi:10.17125/gov2018.ch13.

Buijsman, M.C., B.K. Arbic, J.G. Richman, J.F. Shriver, A.J. Wallcraft, and L. Zamudio, 2017. Semidiurnal internal tide incoherence in the equatorial Pacific. *Journal of Geophysical Research Oceans* 122, 5286-5305, doi: 10.1002/2016JC012590.

Buijsman, M.C., G.R. Stephenson, J.K. Ansong, B.K. Arbic, J.A.M. Green, J.G. Richman, J.F. Shriver, C. Vic, A.J. Wallcraft, and Z. Zhao (2020), On the interplay

between horizontal resolution and wave drag and their effect on tidal baroclinic mode waves in realistic global ocean simulations. *Ocean Modelling*, in review.

Carrier, M.J., H.E. Ngodock, S.R. Smith, I. Souopgui, and B. Bartels, 2016: Examining the Potential Impact of SWOT Observations in an Ocean Analysis-Forecasting System. *Monthly Weather Review* 144, 3767-3782, doi:10.1175/MWR-D-15-0361.1.

Chassignet, E.P., H.E. Hurlburt, E.J. Metzger, O.M. Smedstad, J. Cummings, G.R. Halliwell, R. Bleck, R. Baraille, A.J. Wallcraft, C. Lozano, H.L. Tolman, A. Srinivasan, S. Hankin, P. Cornillon, R. Weisberg, A. Barth, R. He, F. Werner, and J. Wilkin, 2009: U.S. GODAE: Global Ocean Prediction with the HYbrid Coordinate Ocean Model (HYCOM). *Oceanography* 22, 64-75.

Chassignet, E.P., and X. Xu, 2017. Impact of horizontal resolution ($1/12^\circ$ to $1/50^\circ$) on Gulf Stream separation, penetration, and variability. *Journal of Physical Oceanography* 47, 1999-2021, doi: : 10.1175/JPO-D-17-0031.1.

Cummings, J.A., 2005: Operational multivariate ocean data assimilation. *Quarterly Journal of the Royal Meteorological Society* 131, 3583-3604, doi:10.1256/qj.05.105.

Luecke, C.A., B.K. Arbic, J.G. Richman, J.F. Shriver, M.H. Alford, J.K. Ansong, S.L. Bassette, M.C. Buijsman, D. Menemenlis, R.B. Scott, P.G. Timko, G. Voet, A.J. Wallcraft, and L. Zamudio (2020), Statistical comparisons of temperature variance and kinetic energy in global ocean models and observations: Results from mesoscale to internal wave frequencies. *Journal of Geophysical Research Oceans* 125, e2019JC015306, doi:10.1029/2019JC015306.

Mazloff, M.R., B. Cornuelle, B., S.T. Gille, and J. Wang (2020), The importance of remote forcing for regional modeling of internal waves. *Journal of Geophysical Research Oceans* 125, e2019JC015623, doi:10.1029/2019JC015623.

McDougall, T., & Barker, P. (2011). Getting started with TEOS-10 and the Gibbs Seawater (GSW) oceanographic

Nelson, A.D., B.K. Arbic, E.D. Zaron, A.C. Savage, J.G. Richman, M.C. Buijsman, and J.F. Shriver (2019), Toward realistic nonstationarity of semidiurnal baroclinic tides in a hydrodynamic model. *Journal of Geophysical Research Oceans* 124, 6632-6642 doi:10.1029/2018JC014737.

Nelson, A.D., B.K. Arbic, D. Menemenlis, W.R. Peltier, M.H. Alford, N. Grisouard, and J.M. Klymak (2020), Improved internal wave spectral continuum in a regional ocean model. *Journal of Geophysical Research Oceans* 125, e2019JC015974, doi:10.1029/2019JC015974.

Ngodock, H.E., I. Souopgui, A.J. Wallcraft, J.G. Richman, J.F. Shriver, and B.K. Arbic, 2016. On improving the accuracy of the M_2 barotropic tides embedded in a high-resolution global ocean circulation model. *Ocean Modelling* 97, 16-26, doi:10.1016/j.ocemod.2015.10.011.

- Ray, R. D., and D. A. Byrne, 2010: Bottom pressure tides along a line in the southeast Atlantic Ocean and comparisons with satellite altimetry. *Ocean Dynamics* 60, 1167–1176, doi:10.1007/s10236-010-0316-0.
- Richman, J.G., B.K. Arbic, J.F. Shriver, E.J. Metzger, and A.J. Wallcraft, 2012. Inferring dynamics from the wavenumber spectra of an eddying global ocean model with embedded tides. *Journal of Geophysical Research* 117, C12012, doi:10.1029/2012JC008364.
- Rocha, C.B., T.K. Chereskin, S.T. Gille, and D. Menemenlis, 2016a: Mesoscale to submesoscale wavenumber spectra in Drake Passage. *Journal of Physical Oceanography* 46, 601-620, doi:10.1175/JPO-D-15-0087.1.
- Savage, A.C., B.K. Arbic, M.H. Alford, J.K. Ansong, J.T. Farrar, D. Menemenlis, A.K. O'Rourke, J.G. Richman, J.F. Shriver, G. Voet, A.J. Wallcraft, and L. Zamudio, 2017. Spectral decomposition of internal gravity wave sea surface height in global ocean models. *Journal of Geophysical Research Oceans* 122, 7803-7821, doi:10.1002/2017JC013009.
- Schindelegger, M., J. Green, S.-B. Wilmes, and I. Haigh (2018), Can we model the effect of observed sea level rise on tides?, *Journal of Geophysical Research: Oceans* 123 , doi:10.1029/2018JC013959.
- Shriver, J.F., B.K. Arbic, J.G. Richman, R.D. Ray, E.J. Metzger, A.J. Wallcraft, and P.G. Timko, 2012: An evaluation of the barotropic and internal tides in a high resolution global ocean circulation model. *Journal of Geophysical Research* 117, C10024, doi:10.1029/2012JC008170.
- Yu, X., A.L. Ponte, S. Elipot, D. Menemenlis, E.D. Zaron, and R. Abernathy, 2019: Surface kinetic energy distributions in the global oceans from a high-resolution numerical model and surface drifter observations. *Geophysical Research Letters* 46, 9757–9766, doi:10.1029/2019GL083074.
- Zaron, E.D., 2017: Mapping the nonstationary internal tide with satellite altimetry. *Journal of Geophysical Research Oceans* 122, 539–554, doi:10.1002/2016JC012487.